



Molecular Crystals and Liquid Crystals

Publication details, including instructions for authors and subscription information:

<http://www.tandfonline.com/loi/gmcl20>

SELF-ASSEMBLY OF AN IONIC LIQUID AND A HYDROXYL-TERMINATED LIQUID CRYSTAL: ANISOTROPIC ION CONDUCTION IN LAYERED NANOSTRUCTURES

Masafumi Yoshio^a, Takashi Kato^a, Tomohiro Mukai^b, Masahiro Yoshizawa^b & Hiroyuki Ohno^b

^a Department of Chemistry and Biotechnology, School of Engineering, The University of Tokyo, Hongo, Bunkyo-ku, Tokyo 113-8656, Japan

^b Department of Biotechnology, Tokyo University of Agriculture and Technology, Koganei, Tokyo 184-8588, Japan

Version of record first published: 07 Jan 2010

To cite this article: Masafumi Yoshio, Takashi Kato, Tomohiro Mukai, Masahiro Yoshizawa & Hiroyuki Ohno (2004): SELF-ASSEMBLY OF AN IONIC LIQUID AND A HYDROXYL-TERMINATED LIQUID CRYSTAL: ANISOTROPIC ION CONDUCTION IN LAYERED NANOSTRUCTURES, *Molecular Crystals and Liquid Crystals*, 413:1, 99-108

To link to this article: <http://dx.doi.org/10.1080/15421400490432632>

PLEASE SCROLL DOWN FOR ARTICLE

Full terms and conditions of use: <http://www.tandfonline.com/page/terms-and-conditions>

This article may be used for research, teaching, and private study purposes. Any substantial or systematic reproduction, redistribution, reselling, loan, sub-licensing, systematic supply, or distribution in any form to anyone is expressly forbidden.

The publisher does not give any warranty express or implied or make any representation that the contents will be complete or accurate or up to date. The accuracy of any instructions, formulae, and drug doses should be independently verified with primary sources. The publisher shall not be liable for any loss, actions, claims, proceedings, demand, or costs or damages whatsoever or howsoever caused arising directly or indirectly in connection with or arising out of the use of this material.

SELF-ASSEMBLY OF AN IONIC LIQUID AND A HYDROXYL-TERMINATED LIQUID CRYSTAL: ANISOTROPIC ION CONDUCTION IN LAYERED NANOSTRUCTURES

Masafumi Yoshio and Takashi Kato*

*Department of Chemistry and Biotechnology, School of Engineering,
The University of Tokyo, Hongo, Bunkyo-ku, Tokyo 113-8656, Japan*

Tomohiro Mukai, Masahiro Yoshizawa, and Hiroyuki Ohno

*Department of Biotechnology, Tokyo University of Agriculture and
Technology, Koganei, Tokyo 184-8588, Japan*

Anisotropic ion-conductive materials have been prepared by self-assembly of a conventional ionic liquid and a hydroxyl-terminated liquid crystal. These assemblies form phase-segregated layered structures on the nanometer scale. Anisotropic ionic conductivities along the direction parallel and perpendicular to the layer have been successfully measured for the sample forming oriented monodomains. The ionic conductivity parallel to the layer ($\sigma_{i||}$) is higher than that perpendicular to the layer ($\sigma_{i\perp}$). The maximal anisotropy ($\sigma_{i||}/\sigma_{i\perp}$) is 2.6×10^3 at 37°C in the smectic B phase.

Keywords: anisotropic ion conduction; ionic liquids; layered nanostructures; liquid crystals; self-assembly

INTRODUCTION

The anisotropy of supramolecular assemblies and liquid crystals for charge and ion transport can be used for future applications as device materials [1-15]. On the other hand, organic ionic liquids have attracted much attention for the application as electrolytes in electrochemical devices

Financial support of Grant-in-Aid for Scientific Research on Priority Areas, "Dynamic Control of Strongly Correlated Soft Materials" (No. 413/13031009) from the Ministry of Education, Culture, Sports, Science, and Technology is gratefully acknowledged.

*Corresponding author. Tel.: +81-3-5841-7440, Fax: +81-3-5841-8661, E-mail: kato@chiral.t.u-tokyo.ac.jp

because of their high ionic conductivity, electrochemical stability, and non-volatility [16–20].

The formation of supramolecular assemblies containing ionic liquids may lead to the development of new low-dimensionally ion-active materials. Recently, we have reported on new anisotropic ion-conductive materials consisting of a conventional ionic liquid and hydroxyl-terminated liquid crystals [2,14]. The interactions between the hydroxyl moieties and the ionic liquid stabilize the liquid-crystalline (LC) layered assemblies, which form two-dimensional phase-segregated structures on nanometer scale, as schematically illustrated in Figure 1. Anisotropic ionic conductivities along the direction parallel ($\sigma_{i//}$) and perpendicular ($\sigma_{i\perp}$) to the layer were successfully measured for the sample forming oriented monodomains. The magnitude of anisotropy ($\sigma_{i//}/\sigma_{i\perp}$) in the smectic B (S_B) phase was higher than that in the smectic A (S_A) phase. These results show the existence of the mesogen layers contribute to high anisotropy due to the ordered packing of the ion-insulating mesogens, which leads to the lowering of $\sigma_{i\perp}$ [14].

In the present study, the LC layered assemblies of mesogenic molecule **1** and ionic liquid **2** have been prepared (Figure 2). It was expected that the mesogenic molecules with lower clearing points can be used to control the alignment of the assembled materials at ambient temperatures. The LC properties and the ionic conductivities of the mixtures of **1** and **2** have been examined. These materials have been found to exhibit two-dimensional ionic conductivities with high anisotropy at room temperature.

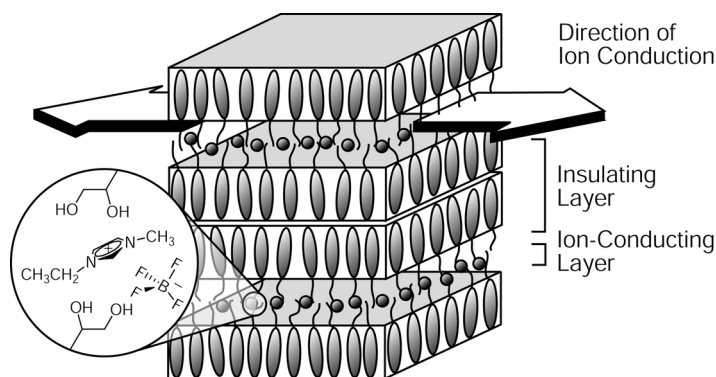
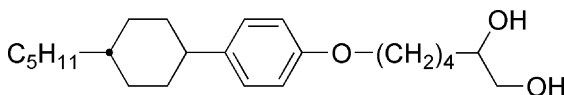
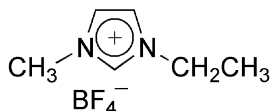


FIGURE 1 Schematic illustration of liquid-crystalline layered assemblies consisting of an ionic liquid and a hydroxyl-terminated mesogenic molecule.



1: Cr 28 S_B 64 S_A 147 Iso (°C)



2: Cr 15 Iso (°C)

FIGURE 2 Molecular structures of mesogenic molecule **1** and ionic liquid **2** and their phase transition behavior. Iso = isotropic, Cr = crystalline, S_A, S_B = smectic A and B.

RESULTS AND DISCUSSION

Liquid-Crystalline Properties

The thermal behavior of the self-assembled materials based on **2** was investigated by differential scanning calorimetry (DSC) and polarizing microscopy. Figure 3 shows a phase diagram for the mixture of **1** and **2** as a function of the mole fraction of **2** on cooling. Compound **1** alone shows enantiotropic smectic phases (S_A and S_B) below ca. 150°C. It is miscible with **2** up to the mole fraction of 0.6 for **2** in the mixture. The transition temperatures from the crystalline phase to the S_B phase become lower with increasing the concentration of **2** though no changes of the LC phases are observed. It is considered that the incorporation of the fluid ionic liquid into the hydrogen-bonded layer reduces the crystallinity of **1**. Similar thermal stabilization of the LC phase by the introduction of **2** is observed in our previous study [14], wherein the LC phase for the mixture consisting of a three-ring mesogenic molecule and **2** is vitrified without crystallizing. The formation of S_A phases for such mixtures was also observed for imidazoles and hydroxyl mesogenic compounds [21].

X-Ray Diffraction Measurements

X-ray diffraction measurements of the mixture of **1** and **2** have been carried out to examine the mesomorphic phase structures. For compound **1**, a set of Bragg peaks at scattering angles with a ratio of 1:1/2:1/3 is observed, which indicates the formation of a well-organized layer of the S_A phase. The layer spacing is 43.7 Å. The length of the mesogenic molecule in

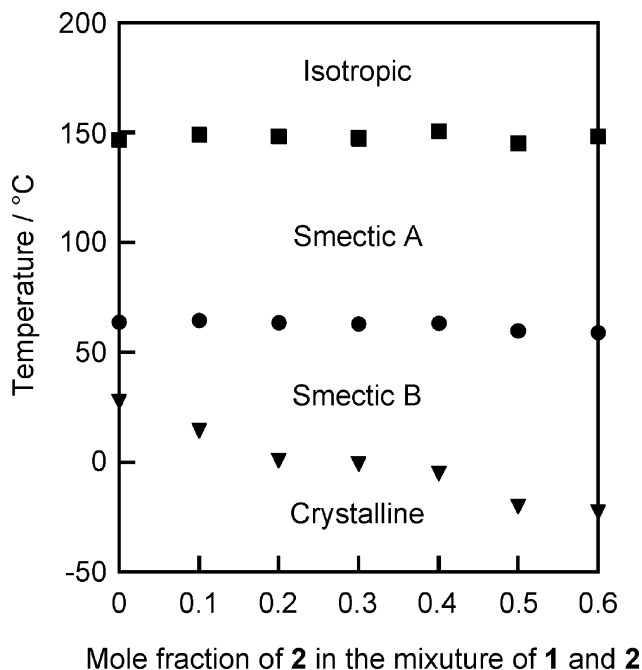


FIGURE 3 Phase transition behavior for a mixture of **1** and **2** on cooling.

the extended conformation is estimated to be 23 Å by molecular modeling. The layer spacing (43.7 Å) of **1** indicates the formation of a bilayer molecular packing through hydrogen bonding between the hydroxyl moieties. For the mixture, the similar diffraction pattern to that of **1** is observed at the same temperature and the layer spacing is 44.1 Å. The layer spacing is slightly extended for the mixture due to the incorporation of the ionic layer. The possible structure of the self-assembled mixtures of **1** and **2** is illustrated in Figure 4. The ionic liquid is stabilized and located in the polar environment yielded by self-association of hydroxyl moieties. The formation of such phase-segregated layer structure on nanometer scale plays a key role for anisotropic ion conduction [2].

Ionic Conductivities

The anisotropic ionic conductivities of the self-assembled mixture of **1** and **2** have been measured by an alternating current impedance method on heating. The details of the experimental procedures were described in our previous paper [10,11]. The cells used for the anisotropic measurements are shown in Figure 5. Cell A consists of a glass plate on which

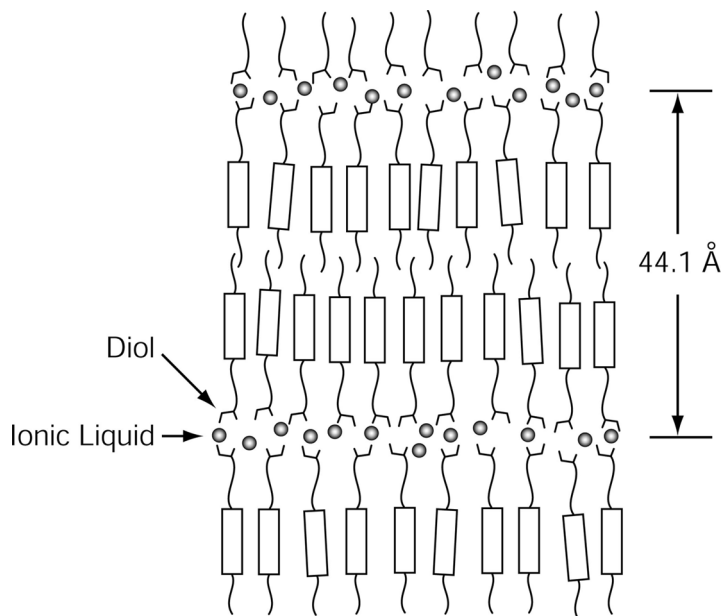


FIGURE 4 Self-assembled nanostructure for the mixture of **1** and **2** in the S_A phase.

comb-shaped gold electrodes are vapor-deposited. The mixtures filled in the cell show homeotropic alignment in the smectic phases. The orientation has been confirmed by conoscopic observation on a polarizing microscope. For cell A filled with oriented samples, the ionic conductivities parallel to the layer direction of the smectic phases can be measured. For cell B that consists of a pair of indium tin oxide (ITO) electrodes, the mixtures also form a homeotropically aligned monodomain. The ionic conductivities perpendicular to the layer direction of the smectic phases can be obtained by using cell B.

Figure 6 shows the anisotropic ionic conductivities of the self-assembled mixture of **1** and **2** in the molar ratio of 8:2 as a function of temperature. The ionic conductivity parallel to the smectic layer (\bullet) is higher than that perpendicular to the layer (\circ). The highest value of $\sigma_{i//}$ is $4.8 \times 10^{-4} \text{ S cm}^{-1}$ in the S_A phase at 122°C . The magnitude of anisotropy at the same temperature is 5.0. The magnitude of maximal anisotropy is 2.6×10^3 in the S_B phase at 37°C . The anisotropy of the ion conduction in the S_B phase is higher than that in the S_A phase. In the S_B phase, the hexagonal ordered packing of the mesogen may effectively disturb the ion conduction perpendicular to the layer. No anisotropy of the ionic conductivity is observed when the liquid-crystalline order disappears at the isotropization

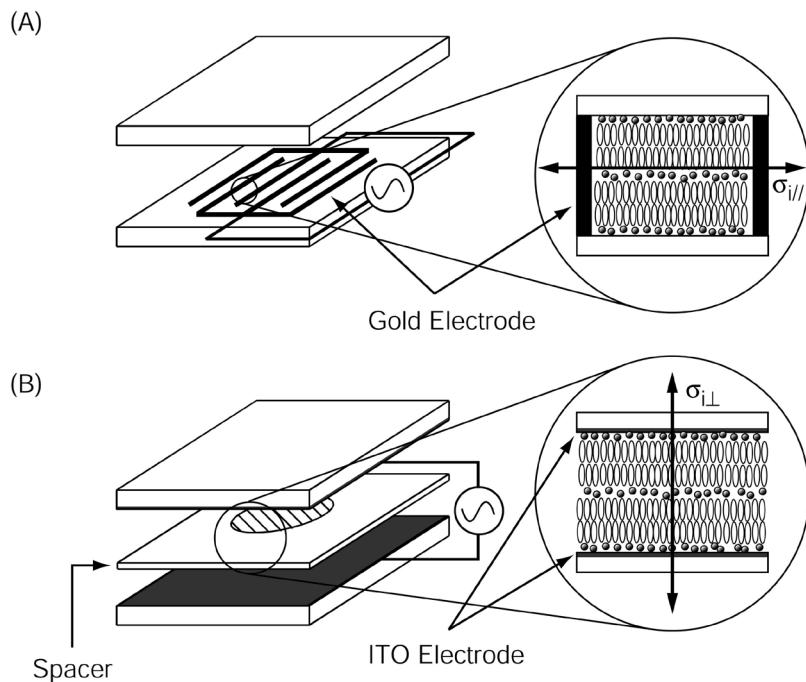


FIGURE 5 Schematic illustrations of the cells used for anisotropic ionic conductivity measurements: (A) comb-shaped gold electrodes and (B) ITO electrodes. The arrows show the direction of conductivity measurements.

temperature on heating. The formation of the smectic layered structure through the nanophase segregation between **1** and **2** results in the spontaneous formation of an anisotropic ion-conductive pathway with long-range order. In order to obtain high ion-conductive LC materials, the concentration of **2** in the assembled materials is increased.

The ionic conductivities ($\sigma_{i//}$) for the oriented mixtures of **1** and **2** in the molar ratio of 7:3 (\blacktriangle), 8:2 (\bullet), and 9:1 (\blacksquare) are shown in Figure 7. The increase of the mole fraction of **2** in the mixture results in the increase of ionic conductivities of the materials. It is assumed that the increase of the mobile ions without anchoring from mesogenic molecules enhances the ion conduction in layered nanostructures.

CONCLUSION

The use of interactions between a conventional ionic liquid and hydroxyl-terminated mesogenic compound leads to the formation of self-assembled

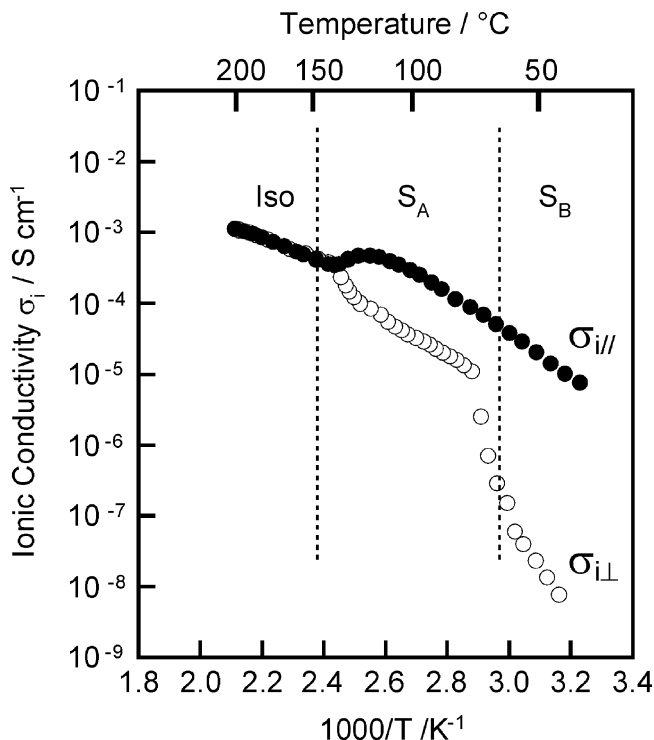


FIGURE 6 Ionic conductivities of the self-assembled mixture of **1** and **2** in the molar ratio of 8:2.

anisotropic ion-conductive materials. We have succeeded in the anisotropic measurements of ionic conductivity by controlling the molecular alignment of the materials. The ionic conductivities of the materials are tunable by the change of the fraction of ionic liquid or by proper design of the components. These materials should be widely applicable to electrochemical devices.

EXPERIMENTAL

Characterization

DSC measurements were performed with a Mettler DSC 30 at a scanning rate of $10^{\circ}\text{C min}^{-1}$. Polarizing microscope observations were conducted with an Olympus BX51 microscope equipped with a Mettler FP82 hot stage. Small angle X-ray diffraction patterns were measured with a Rigaku RINT

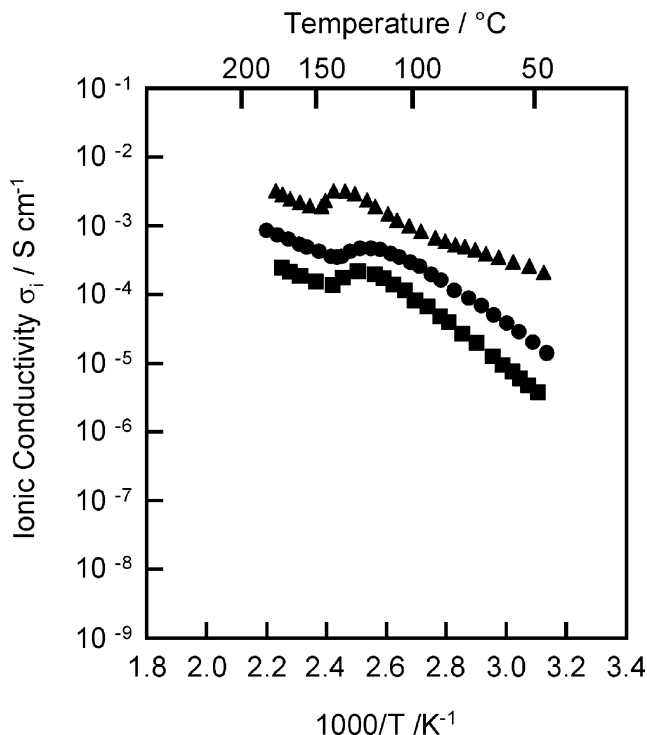


FIGURE 7 Ionic conductivities along the direction parallel ($\sigma_{i||}$) to the smectic layer for the oriented mixtures of **1** and **2** in the molar ratio of 7:3 (▲), 8:2 (●), and 9:1 (■).

2100 diffractometer. The scattered radiation was collected on a 2D imaging plate system (Rigaku, R-Axis DS3C).

6-[4-(*trans*-4-Pentylcyclohexyl)Phenoxy]Hexane-1,2-diol (**1**)

4-(*trans*-4-Pentylcyclohexyl)phenol (Kanto Chemicals) (2.00 g, 8.12 mmol) and triphenylphosphine (3.20 g, 12.2 mmol) were dissolved in dry tetrahydrofuran (20 mL). After addition of 1,2-*O*-isopropylidenehexane-1,2,6-triol [22,23] (1.74 g, 10.0 mmol) the mixture was cooled to 0°C. At this temperature diethylazodicarboxylate (2.09 g, 12.0 mmol) was added dropwise over 10 min to the stirred mixture, and the solution was stirred for an additional 10 h at room temperature. Then the solvent was evaporated and the residue was dissolved in hexane. An insoluble triphenylphosphine oxide was filtered off through a pad of Celite by using a suction funnel and the solvent was evaporated. The residue was dissolved in wet ethanol

(50 mL, containing 5% water). After addition of *p*-toluenesulfonic acid monohydrate (1.72 g, 10.0 mmol) the solution was refluxed for 3 h. Removal of the solvent *in vacuo* gave a residue, which was dissolved in ethyl acetate (50 mL) and washed with water and brine successively. The resulting organic phase was dried over sodium sulfonate, filtered, and evaporated under reduced pressure. The residue was purified by flash column chromatography on silica gel (eluent: chloroform-methanol = 20:1, R_f = 0.34) and recrystallization from hexane to give **1** in a yield of 71% (2.09 g, 5.77 mmol). mp = 94°C. ^1H NMR (400 MHz, CDCl_3): δ = 0.89 (t, J = 7 Hz, 3H), 1.01–2.05 (m, 17H), 2.40 (tt, J = 4, 12 Hz, 1H), 3.45 (m, 1H), 3.66 (m, 1H), 3.74 (m, 1H), 3.94 (t, J = 6 Hz, 2H), 6.81 (d, J = 9 Hz, 2H), 7.11 (d, J = 9 Hz, 2H). ^{13}C NMR (100 MHz, CDCl_3): δ = 14.1, 22.2, 22.7, 26.6, 29.2, 32.2, 32.8, 33.6, 34.5, 37.3, 37.4, 43.7, 66.7, 67.6, 72.1, 114.2, 127.6, 140.1, 157.0. Elemental analysis calcd. for $\text{C}_{23}\text{H}_{38}\text{O}_3$: C, 76.20; H, 10.56%. Found: C, 75.88; H, 10.43%.

1-Ethyl-3-methylimidazolium tetrafluoroborate (2)

Ionic liquid **2** was prepared according to the procedure described by Fuller *et al.* [24].

Preparation of Ionic Liquid Mixtures

All mixtures examined in the present study were prepared by slow evaporation from dichloromethane solution containing the requisite amounts of **1** and **2** followed by drying *in vacuo* at 25°C for 5 h.

Measurements of Ionic Conductivity

Dynamic ionic conductivities were measured by using an impedance analyzer (Schlumberger, Solartron 1260) and a custom set-up temperature controller.

REFERENCES

- [1] Demus, D., Goodby, J. W., Gray, G. W., Spiess, H.-W., & Vill, V. (Eds.) (1998). *Handbook of Liquid Crystals*, Wiley-VCH, Weinheim.
- [2] Kato, T. (2002). *Science*, 295, 2414.
- [3] van Nostrum, C. F. & Nolte, R. J. M. (1996). *Chem. Commun.*, 2385.
- [4] van Nostrum, C. F., Picken, S. J., Schouten, A.-J., & Nolte, R. J. M. (1995). *J. Am. Chem. Soc.*, 117, 9957.
- [5] Adam, D., Schuhmacher, P., Simmerer, J., Häussking, L., Siemensmeyer, K., Etzbach, K. H., Ringsdorf, H., & Haarer, D. (1994). *Nature*, 371, 141.

- [6] Boden, N., Bushby, R. J., & Clements, J., (1993). *J. Chem. Phys.*, *98*, 5920.
- [7] Mizoshita, N., Monobe, H., Inoue, M., Ukon, M., Watanabe, T., Shimizu, Y., Hanabusa, K., & Kato, T. (2002). *Chem. Commun.*, 428.
- [8] Percec, V., Heck, J. A., Tomazos, D., & Ungar, G. (1993). *J. Chem. Soc Perkin*, *2*, 2381
- [9] Smith, R. C., Fischer, W. M., & Gin, D. L. (1997). *J. Am. Chem. Soc.*, *119*, 4092.
- [10] Ohtake, T., Ito, K., Nishina, N., Kihara, H., Ohno, H., & Kato, T. (1999). *Polym. J.*, *31*, 1155.
- [11] Ohtake, T., Ogasawara, M., Ito-Akita, K., Nishina, N., Ujiie, S., Ohno, H., & Kato, T. (2000). *Chem. Mater.*, *12*, 782.
- [12] Ohtake, T., Takamitsu, Y., Ito-Akita, K., Kanie, K., Yoshizawa, M., Mukai, T., Ohno, H., & Kato, T. (2000). *Macromolecules*, *33*, 8109.
- [13] Ohtake, T., Kanie, K., Yoshizawa, M., Mukai, T., Ito-Akita, K., Ohno, H., & Kato, T. (2001). *Mol. Cryst. Liq. Cryst.*, *364*, 589.
- [14] Yoshio, M., Mukai, T., Kanie, K., Yoshizawa, M., Ohno, H., & Kato, T. (2002). *Adv. Mater.*, *14*, 351.
- [15] Yoshio, M., Mukai, T., Kanie, K., Yoshizawa, M., Ohno, H., & Kato, T. (2002). *Chem. Lett.*, 320.
- [16] Welton, T. (1999). *Chem. Rev.*, *99*, 2071.
- [17] Bonhôte, P. Dias, A.-P., Papageorgiou, N., Kalyanasundaram, K., & Grätzel, M. (1996). *Inorg. Chem.*, *35*, 1168.
- [18] MacFarlane, D. R., Meakin, P., Sun, J., Amini, N., & Forsyth, M. (1999). *J. Phys. Chem. B*, *103*, 4164.
- [19] Ohno, H. (2001). *Electrochim. Acta*, *46*, 1407.
- [20] Yoshizawa, M., Hirao, M., Ito-Akita, K., & Ohno, H. (2001). *J. Mater. Chem.*, *11*, 1057.
- [21] Kato T. & Kawakami, T. (1997). *Chem. Lett.*, 211.
- [22] Hentrich, F., Tschierske, C., Diele, S., & Sauer, C. (1994). *J. Mater. Chem.*, *4*, 1547.
- [23] Neumann, B., Sauer, C., Diele, S., & Tschierske, C. (1996). *J. Mater. Chem.*, *6*, 1087.
- [24] Fuller, J., Carlin, R. T., De Long, H. C., & Haworth, D. (1994). *J. Chem. Soc., Chem. Commun.*, 299.